RSC Advances

PAPER

View Article Online
View Journal | View Issue

Cite this: *RSC Adv.*, 2019, **9**, 9694

A large-surface-area TS-1 nanocatalyst: a combination of nanoscale particle sizes and hierarchical micro/mesoporous structures†

Changlin Du,[ab] Nan Cui,[ab] Linghao Li,[ab] Zile Hua *[ab] and Jianlin Shi [ab]

By a simple sequent process of dry-gel steam-assisted crystallization and following a top-down alkali-etching treatment, hierarchically structured TS-1 nanozeolites (nanoTS-1_D) with abundant micro/mesopores have been synthesized for the first time, and they exhibit remarkably high specific surface area of 606 $m^2\ g^{-1}$ and pore volume of 0.86 $cm^3\ g^{-1}$. Characterization by XRD, FTIR, UV-vis and EM confirm the exclusive incorporation of titanium species in zeolite frameworks. More importantly, compared with the microporous TS-1 nanocrystal material with identical particle sizes of 80 nm (nanoTS-1) and submicrometer-sized mesoporous TS-1 material (mesoTS-1), here the reported nanoTS-1_D catalyst shows greatly improved performance in the model reaction of 1-hexene epoxidation. 40.9% olefin conversion and 96.3% epoxide selectivity are achieved and its high stability is verified by the 6 recycling–regeneration tests.

Received 7th January 2019
Accepted 21st March 2019

DOI: 10.1039/c9ra00124g

rsc.li/rsc-advances

1. Introduction

Owing to the high catalytic activity and stability towards many selective oxidation reactions using dilute H_2O_2 solution as the oxidant, the successful synthesis of MFI-type titanosilicate zeolites (TS-1) has been considered as a breakthrough in the field of microporous catalytic materials.[1,2] However, restricted by the small pore size (~0.54 nm in pore width) of the microporous structures, conventional microporous TS-1 materials show limited accessibility to the active titanium species located within the frameworks especially for bulky molecules, which is also a common issue to all types of microporous zeolites.[3] In order to tackle these problems, two major strategies, *i.e.*, decreasing zeolite particle sizes to the nanoscale (nanozeolites)[4,5] and introducing auxiliary mesoporous structures (hierarchical zeolites),[6–8] have been developed and great progress has been made in recent years. It is believed that their superior performances are associated with the shortening of mass diffusion length in the microporous channels and the improved accessibility to the framework active sites.[9,10] Unfortunately, synthesis of nanozeolites often suffers from the low solid yields and the consumption of a large amount of microporous structure-directing agents (SDAs).[11] Meanwhile, additional mesopore templates, such as surfactants,[12,13] carbon materials[14,15] and organosilanes[16,17] are necessarily adopted in the conventional synthesis of hierarchical zeolites. Based on the micro-/mesopore bi-functional diquaternary ammonium surfactant template design, Ryoo *et al.* reported a pioneering work on the preparation of single-unit-cell zeolite.[18,19] The resultant TS-1 nanosheets showed high specific surface area of 580 $m^2\ g^{-1}$ and notable catalytic activities with high epoxide selectivity for bulky olefin epoxidation.[19] Very recently, Yu *et al.* prepared anatase-free nanosized hierarchical TS-1 zeolites by using Triton X-100 as mesoporous template under rotational crystallization conditions, which exhibits high catalytic performance in the alkene epoxidation reactions, *e.g.*, 1-hexene.[20] However, all these processes involve a large amount of commercial or home-made mesoporous template agents, which not only increase the cost of synthesis, but also result in the significant emission of greenhouse gas during the subsequent template elimination. On the other hand, as an alternative, post-synthesis demetallation through acid/alkali/steaming treatment or a combined process has been developed to be a general and facile approach for the preparation of aluminosilicate hierarchical zeolites.[21–23] Different from negatively charged aluminosilicate frameworks, TS-1 zeolites possess the neutral frameworks due to the equal valent substitution of Si by Ti. Thus, the post-synthesis alkali-etching treatment on TS-1 zeolites leads to nonselective removal between Si and Ti species from the framework in the same step, which implies that the variation of framework chemical compositions before and after alkali-etching treatment is controllable, as reported by Tuel *et al.* in preparing hollow TS-1 crystals through post-synthesis treatment with aqueous solutions of

[a]State Key Lab of High Performance Ceramics and Superfine Microstructure, Shanghai Institute of Ceramics, Chinese Academy of Sciences, Shanghai 200050, China. E-mail: huazl@mail.sic.ac.cn

[b]Centre of Materials Science and Optoelectronics Engineering, University of Chinese Academy of Sciences, Beijing 100049, China

† Electronic supplementary information (ESI) available. See DOI: 10.1039/c9ra00124g

tetrapropylammonium hydroxide.[23] Moreover, it is suggested that the dissolution/recrystallization process helps the reincorporation of extra-framework Ti species into the zeolite frameworks, which contributes to the improvement of materials catalytic activity. In the report of Gläser *et al.*, a two-step desilication and surfactant-assisted recrystallization approach was adopted for preparing nanosized TS-1 with micro-/mesoporosity.[24] The resultant material shows specific surface area of 503 $m^2\ g^{-1}$ and enhanced activity in the epoxidation of the unsaturated fatty acid methyl esters (FAME) with H_2O_2. Though highly facile and effective, there are still extremely few reports of preparation of hierarchical TS-1 zeolites using such a post-etching treatment, which is expected here to be applicable for the synthesis of hierarchically structured TS-1 nanozeolites with ever-larger specific surface area and much enhanced catalytic activity.

In our previous report, TS-1 nanozeolites (nanoTS-1) with uniform and adjustable particle sizes have been successfully prepared *via* a dry-gel steam-assisted crystallization (SAC) procedure.[25] Herein, by a combination with post-synthesis alkali-etching treatment, hierarchically structured TS-1 nanozeolites (nanoTS-1_D) with abundant micro-/mesopores have been synthesized for the first time, which exhibit an extremely high specific surface area of 606 $m^2\ g^{-1}$ and total pore volume of 0.86 $cm^3\ g^{-1}$, even higher than those of reported TS-1 nanosheets.[19] Importantly, this unique material exhibits elevated catalytic activity in 1-hexene epoxidation, which is superior to the conventional micrometer-sized TS-1 (microTS-1), nanoTS-1 precursors with identical particle sizes of 80 nm, and submicrometer-sized mesoporous TS-1 materials (mesoTS-1) synthesized by direct hydrothermal process with the assistance of cetyltrimethyl-ammonium bromide (CTAB) surfactant and ethanol.[13]

2. Experimental

2.1. Catalysts preparation

2.1.1 Nano-crystalline TS-1 zeolite. Nano-crystalline TS-1 zeolites were synthesized according to the steam-assisted crystallization process with a permanent Si/Ti molar ratio of 50 by controlling the molar ratio of tetraethyl orthosilicate (TEOS) and tetrabutyl titanate (TBOT) in the preparation process.[25] In the typical synthesis, 10.98 g of tetrapropylammonium hydroxide (TPAOH, 25 wt%) was added dropwise into 10.42 g of TEOS together with 18 g of deionized water to obtain an aqueous solution. The mixture was stirred at 40 °C for 4 h. Then, 0.34 g of TBOT dissolved in 6 g of isopropanol was added dropwise to the mixture and stirred below 4 °C for another 4 h, which makes Ti incorporated into silicon tetrahedron. The mixture was stirred at 40 °C for 48 h to get the solid precursor gel, then crystallized at 180 °C for 10 h. After repeated centrifugation, rinsing with deionized water and drying at 70 °C overnight, the precursor was calcined in air at 550 °C for 6 h to get nano-crystalline TS-1 zeolite (denoted as nanoTS-1).

2.1.2 Hierarchically structured nano-crystalline TS-1 zeolite. The alkali-etching procedure of nanoTS-1 was according to the methodology reported by Groen *et al.*[30] The as-synthesized nanoTS-1 sample was treated with alkaline solution of NaOH and TPAOH. In the typical preparation, 2.5 g of nanoTS-1 was added into 75 ml of alkaline solution (0.08 M NaOH/0.12 M TPAOH). Then, the mixture was stirred at 65 °C for 30 min. After rapid cooling, repeated centrifugation, rinsing with deionized water to neutral, the sample was dried at 80 °C for 12 h. The obtained sample was mixed under stirring with 250 ml of aqueous HCl solution (0.1 M). Then, the mixture was stirred at 65 °C for 6 h. After rapid cooling, repeated centrifugation, rinsing with deionized water to neutral, the sample was dried at 80 °C for another 12 h. Finally, after calcined in air at 540 °C for 5 h, hierarchically structured nano-crystalline TS-1 zeolite was obtained (denoted as nanoTS-1_D).

2.2. Catalyst characterization techniques

The XRD patterns were obtained on Rigaku D/Max 2200PC powder X-ray diffractometer with $Cu_{K\alpha}$ radiation source (λ = 0.15418 nm). The X-ray tube was operated at 40 kV, 40 mA; the two-theta angle was scanned from 5° to 50° (angular step wise 0.02°) at a speed of 5° min^{-1}. The surface area and pore size distribution of the catalysts were characterized on an automatic N_2 adsorption–desorption instrument (TriStar II 3020) at 77 K. The specific surface areas of the samples were calculated by the Brunauer–Emmett–Teller (BET) method and pore size distribution by the Barrett–Joyner–Halenda (BJH) model in the sorption branches of the isotherms. Before the measurement, the samples were dried at 150 °C for 5 h. Diffuse reflectance UV-vis spectra of the samples were recorded from 190 to 800 nm using a Shimadzu UV-310PC spectrometer with $BaSO_4$ as a reference. And silicon, titanium contents of the catalysts were measured by optical emission spectrometry with inductively coupled plasma (ICP-OES) on Agilent 725. Field-emission scanning electron microscopy (FE-SEM) measurements of the samples were characterized on HITACHI SU8220. Besides, Transmission Electron Microscopy (TEM) pictures were carried out on JEM-2100F electron microscope equipped with a field emission source operating at 200 kV. The FT-IR spectra were obtained on a Fourier Transform Infrared Spectroscopy (FT-IR) measurement FTIR-7600 to analyze the existence form and coordination status of titanium.

2.3. Catalytic evaluation

The epoxidation of 1-hexene with H_2O_2 (30 wt% aqueous solution) was carried out in a three-necked round-bottomed flask equipped with a reflux condenser. Typically, 50 mg of catalyst, 10 ml of methanol, 10 mmol of 1-hexene and 10 mmol of H_2O_2 were mixed in the reactor and stirred vigorously at 60 °C for 4 h. After reaction, the products were characterized on Shimadzu GC/MS-2010 equipped with a Rxi-5Sil MS column and an FID detector. To characterize the catalyst stability, we separated the used nanoTS-1_D by centrifugation and rinsing with deionized water and ethanol after each reaction. Then the recovered catalyst was dried at 70 °C overnight, following by calcined in air at 540 °C for 3 h. Finally, the regenerated nanoTS-1_D (denoted as Re. nanoTS-1_D) was obtained and kept for next recycling catalytic reaction. 6 recycling regeneration tests have been performed.

3. Results and discussion

3.1. Catalysts characterization

3.1.1 XRD analysis. The powder X-ray diffraction (XRD) patterns of synthesized TS-1 zeolites are presented in Fig. 1A. All of them reveal the typical Bragg diffraction peaks of MFI-type zeolites. Meanwhile, the absence of diffraction peak at 2θ of 25.40°, which is associated with the (101) plane of TiO_2 anatase phases, confirms that XRD-detectable extra-framework titanium is absent in the resultant materials and titanium is incorporated into the siliceous zeolite framework. More evidences could be found in the following spectroscopic analyses (UV-vis spectra of Fig. 1B of and FT-IR spectra of Fig. S3†). Except for sample nanoTS-1_D, the comparable high-intensity diffraction peaks with the other three samples prove their high crystallinity. About nanoTS-1_D, a reduction in the diffraction intensity could be resulted from the auxiliary intracrystal mesoporous structures which improve the mass transfer in the hierarchical zeolites, but as an artificial defect break the intrinsic periodic structure of microporous zeolite crystals.[24] In the meantime, the coordination status of Ti species was also characterized by UV-vis spectrometer, as shown in Fig. 1B. All TS-1 materials present an obvious absorbance at 220 nm ascribed to the charge transition from O(2p) to Ti(3d),[26] which clearly demonstrates that most of Ti species have been tetrahedrally coordinated in the siliceous zeolite framework. It should be noted that a weak absorption edge onset appears at ~320 nm (the inset dashed rectangle) in samples nanoTS-1 and mesoTS-1, which is associated with titanium-enriched species or titania nanoclusters, verifying the presence of extra-framework Ti species in the samples, though it is undetectable with XRD characterization. In contrast, such a weak absorption edge is not visible for sample nanoTS-1_D, which means that the extra-framework titanium species has been removed through the post-synthesis alkali-etching process. As a result, a slightly increased Si/Ti molar ratio from 72 to 82 is obtained for sample nanoTS-1_D, as listed in Table 1. The clear adsorption band at 960 cm^{-1} in Fig. S3† of FT-IR spectra, which is assigned to the stretching vibration of Ti–O–Si bond, provides an additional proof for the successful incorporation of Ti into synthesized zeolite frameworks in the samples.[2,27,28]

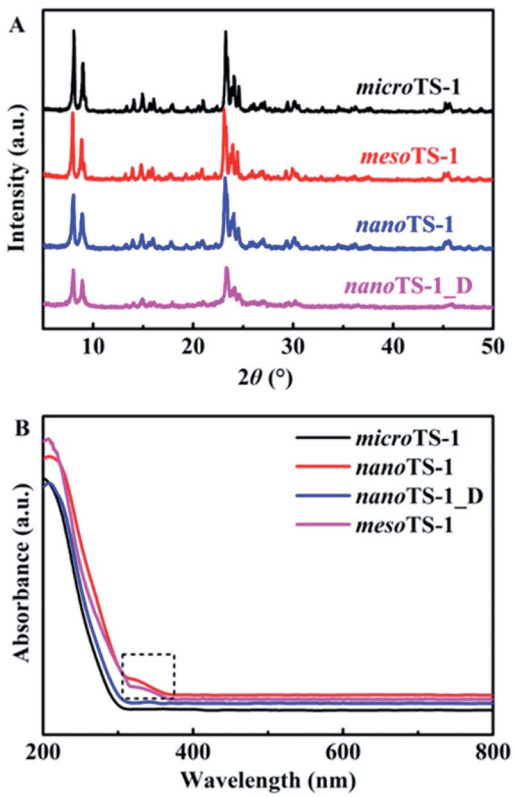

Fig. 1 (A) Powder XRD patterns and (B) UV-vis spectra of synthesized TS-1 zeolites.

3.1.2 Nitrogen sorption/desorption analysis. The N_2 sorption isotherms and BJH pore size distributions (PSD) of the synthesized TS-1 zeolites are shown in Fig. 2, and their textural properties are summarized in Table 1. As expected, microTS-1 zeolite shows the typical type I profile of microporous materials with a high uptake at low relative pressures ($P/P_0 < 0.1$) and a plateau at high relative pressures. Consequently, its PSD plot based on the adsorption branch demonstrates the peak absence in the mesopore range of 2.0–100 nm. The corresponding specific surface area and total pore volume are 420 $m^2\ g^{-1}$ and 0.22 $cm^3\ g^{-1}$, respectively. For sample nanoTS-1 and mesoTS-1, the type IV isotherms are present and the apparent uptake steps at P/P_0 of 0.90 and 0.40 respectively reflects their specific intercrystal and intracrystal mesoporous structures, which are in agreement with previous reports.[13,25] Interesting results are found for alkali-etched sample nanoTS-1_D. Compared to that of nanoTS-1 precursors, besides the hysteresis loop and steep rise at the high relative pressures of 0.80–0.99 associated with the intercrystal mesopores, the N_2 sorption volume is significantly increased in the whole pressure range and a new hysteresis loop appears at the relative pressures between 0.45–0.70, indicating the formation of new mesoporous structures. A double-peak distribution is observed in its PSD plot, in which the mesopores centred at *ca.* 44.3 nm are the intercrystal mesovoids and the newly appeared small peak centred at *ca.* 3.8 nm corresponds to the alkali-etching generated intracrystal mesopores. As listed in Table 1, sample nanoTS-1_D possesses the highest specific surface area of 606 $m^2\ g^{-1}$ and total pore volume of 0.86 $cm^3\ g^{-1}$, which are respectively 122 $m^2\ g^{-1}$ and 0.44 $cm^3\ g^{-1}$ higher than those of nanoTS-1 precursor, and also higher than the corresponding values (specific surface area of 580 $m^2\ g^{-1}$ and total pore volume of 0.61 $cm^3\ g^{-1}$) of single-unit-cell TS-1 nanosheets.[19]

3.1.3 EM analysis. TEM and SEM images provide the direct evidences for the formation of intracrystal mesopores in nanoTS-1_D materials. SEM images of Fig. 3C and S1B† depict that sample nanoTS-1_D consists of highly dispersed and uniform nanocrystals of *ca.* 80 nm, similar to that of nanoTS-1 precursor as shown in Fig. 3A and S1A.† Additionally, the inset histograms of DLS analyses in Fig. S1A and B† show the similar particle size distributions and the mean particle sizes are *ca.* 80 nm. The consistency between SEM and DLS results confirms the negligible effect of alkali-etching treatment on the particle size of TS-1 nanozeolites. On the other hand, there exists

Table 1 Chemical composition and structural characteristics of the synthesized TS-1 zeolites

Sample	Si/Ti[a]	S_{BET} (m^2 g^{-1})	S_{exter} (m^2 g^{-1})	V_{total} (cm^3 g^{-1})	V_{meso} (cm^3 g^{-1})
microTS-1	75	420	136	0.22	0.10
mesoTS-1	64	511	351	0.36	0.29
nanoTS-1	72	484	202	0.42	0.30
nanoTS-1_D	82	606	346	0.86	0.74

[a] Si/Ti molar ratio in the bulk determined by ICP.

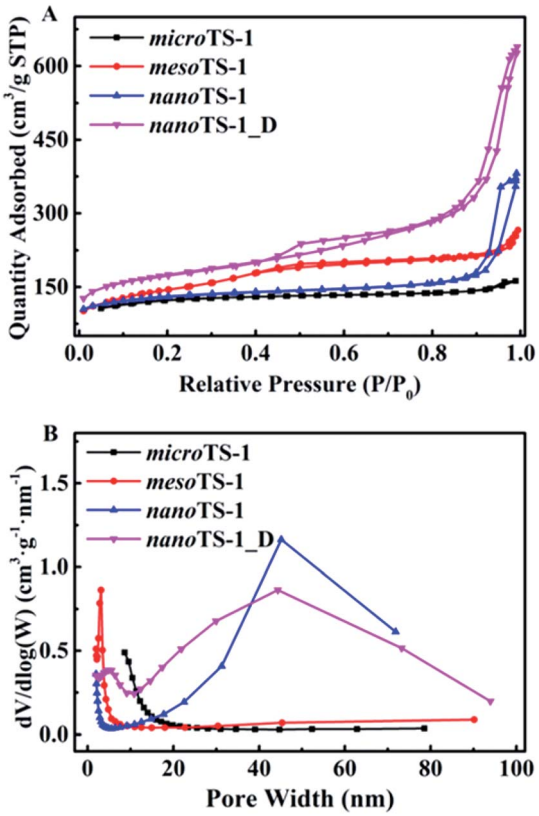

Fig. 2 (A) N_2 sorption isotherms and (B) PSD of synthesized TS-1 zeolites.

significant difference on the particle morphology between synthesized nanoTS-1 and nanoTS-1_D, *i.e.*, compared to the smooth surface of nanoTS-1, the particle surface of nanoTS-1_D is rough with abundant mesopores of about 2.8–4.6 nm on the surface. Moreover, as shown in the TEM images of Fig. 3D, compared to the homogeneous structure of sample nanoTS-1 of Fig. 3B, nanoTS-1_D exhibits much more significant and abundant pore-structures, which is believed to result from the additional mesoporous structures induced by the following alkali-etching treatment. The mesopore sizes are *ca.* 3.5 nm, which are consistent with above N_2 sorption and SEM results.

3.2. Catalytic performance

In the model reaction of 1-hexene epoxidation, all synthesized TS-1 zeolites show the approximately similar product distributions and the target 1,2-epoxyhexane selectivities are larger than 95%, as listed in Table 2. However, their catalytic activities are substantially distinguishable from each other. Since all synthesized TS-1 materials possess the similar Si/Ti ratio (as listed in Table 1), the great difference on catalyst activities should be related to their specific textural properties. Among them, microTS-1 exhibits the lowest 1-hexene conversion of 19.7%, which is in accordance with reported results and confirms the limited accessibility of the reactants to the framework titanium active centres in the conventional microporous catalysts.[29] As expected, the 1-hexene conversions on samples nanoTS-1 and mesoTS-1 are slightly higher at 23.0% and 24.5% respectively because of their auxiliary intercrystal or intracrystal mesoporous structures. Interestingly, benefitting from the extraordinarily high surface area of alkali-etched nanoTS-1, a significantly elevated conversion of 40.9% has been achieved, which is more than twice that of microTS-1. And the calculated TON also certifies the good accessibility of surface titanium active centres in synthesized nanoTS-1_D and consequent high activity. Meanwhile, it should be noted that the extra-framework titanium species would cause the non-catalytic decomposition of H_2O_2 oxidant and are harmful to the catalytic oxidation reactions.[20] As suggested by the above UV-vis results, the elimination of extra-framework Ti species also contributes to the activity enhancement of sample nanoTS-1_D.

In addition, recycling experiments were performed to verify the catalytic stability of synthesized nanoTS-1_D. As shown in Table 2 and S1,† the 1-hexene conversion and 1,2-epoxyhexane selectivity keep almost constant in the consecutive 6 recycling–regeneration tests, demonstrating the high stability of nanoTS-1_D catalysts. Moreover, XRD patterns also indicates the well-

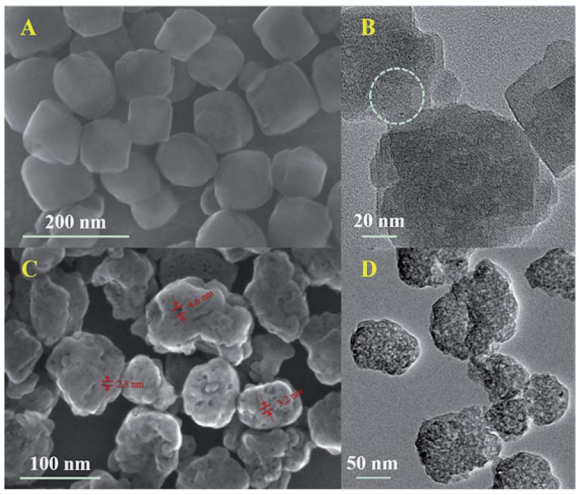

Fig. 3 (A) SEM image and (B) TEM image of synthesized nanoTS-1; (C) SEM image and (D) TEM image of synthesized nanoTS-1_D.

Table 2 Catalytic performances of synthesized TS-1 zeolites in the epoxidation reaction of 1-hexene using H_2O_2[a]

		1-Hexene epoxidation		
Sample	Ti content[b] (wt%)	Conv. (%)	Sel.[c] (%)	TON
microTS-1	1.05	19.7	96.4	180
nanoTS-1	1.09	23.0	95.5	202
mesoTS-1	1.23	24.5	96.5	191
nanoTS-1_D	0.96	40.9	96.3	408
Re. nanoTS-1_D[d]	0.94	40.7	95.9	415

[a] Reaction conditions: 1-hexene, 10 mmol; H_2O_2, 10 mmol; MeOH, 10 ml; catalyst, 50 mg; 60 °C, 4 h. [b] Ti content in the bulk catalysts determined by ICP. [c] The selectivity of 1,2-epoxyhexane. [d] nanoTS-1_D catalyst after 6 recycling–regeneration tests in the epoxidation of 1-hexene under the same reaction condition.

preserved MFI-type structure of nanoTS-1_D after 6 recycling–regeneration (Fig. S3A†). Meanwhile, UV-vis spectra suggest that no anatase TiO_2 is present in the regenerated nanoTS-1_D material (Fig. S3B†). Besides, the N_2 sorption isotherms and BJH PSD results of the regenerated nanoTS-1_D are consistent with those of the original material, indicating the well-maintained hierarchically micro-/mesoporous structure in recycled nanoTS-1_D (Fig. S3C, D and Table S1†). All of these characterization results demonstrate that the large-surface-area nanoTS-1_D zeolite with nanoscale particle size and hierarchically micro-/mesoporous structure is an extremely active and stable catalyst in epoxidation of 1-hexene.

4. Conclusion

In summary, a novel nano-sized and hierarchical micro-/mesoporous structured TS-1 nanocatalyst (nanoTS-1_D) has been prepared by a facile sequent process of dry-gel steam-assisted crystallization and following alkali-etching treatment. The hierarchical nanocatalyst possesses remarkably high specific surface area of 606 $m^2\ g^{-1}$ and total pore volume of 0.86 $cm^3\ g^{-1}$, which are comparable to the previously reported single-unit-cell TS-1 nanosheets. As a result, in the model reaction of 1-hexene epoxidation, nanocatalyst demonstrates 40.9% of olefin conversion and 96.3% of epoxide selectivity, which is superior to the conventional micrometer-sized TS-1 (microTS-1), nanoTS-1 precursors with identical particle sizes of 80 nm, and submicrometer-sized mesoporous TS-1 materials of mesoTS-1. Considering the wide applications of titaniumsilicate zeolites in the selective oxidation reactions, such a facile but efficient two-step strategy for the synthesis of novel-structured TS-1-based catalysts would be of high significance in the fine chemical production and petrochemical industry. Further studies about detailed processes and mechanisms of post-synthesis alkali-etching and its effect on the textural and surface properties of TS-1 and non-aluminum doping silicate zeolites are in progress.

Conflicts of interest

There are no conflicts to declare.

Acknowledgements

This work was sponsored by the National Natural Science Foundation of China (21776297, U1510107).

Notes and references

1 U. Wilkenhöner, G. Langhendries, F. V. Laar, G. V. Baron, D. W. Gammon, P. A. Jacobs and E. V. Steen, *J. Catal.*, 2001, **203**, 201.
2 D. P. Serrano, R. Sanz, P. Pizarro, I. Moreno and S. Medina, *Appl. Catal., B*, 2014, **146**, 35.
3 X. Zhang, D. Liu, D. Xu, S. Asahina, K. A. Cychosz and K. Varoon, *Science*, 2012, **336**, 1684.
4 W. Schwieger, A. G. Machoke, T. Weissenberger, A. Inayat, T. Selvam, M. Klumpp and A. Inayat, *Chem. Soc. Rev.*, 2016, **45**, 3353.
5 P. Bai, E. Haldoupis, P. J. Dauenhauer, M. Tsapatsis and J. I. Siepmann, *ACS Nano*, 2016, **10**, 7612.
6 D. P. Serrano, J. M. Escola and P. Pizarro, *Chem. Soc. Rev.*, 2013, **42**, 4004.
7 B. Li, Z. Hu, B. Kong, J. Wang, W. Li, X. Sun, X. Qian, Y. Yang, W. Shen, H. Xu and D. Zhao, *Chem. Sci.*, 2014, **5**, 1565.
8 M. Milina, S. Mitchell, P. Crivelli, D. Cooke and J. PérezRamírez, *Nat. Commun.*, 2014, **5**, 3922.
9 D. Verboekend and J. Pérez-Ramírez, *Catal. Sci. Technol.*, 2011, **1**, 879.
10 H. Zhang, Z. Hu, L. Huang, H. Zhang, K. Song, L. Wang, Z. Shi, J. Ma, Y. Zhuang, W. Shen, Y. Zhang, H. Xu and Y. Tang, *ACS Catal.*, 2015, **5**, 2548.
11 R. Martinez-Franco, C. Paris, M. E. Cristina, C. Martinez, M. Moliner and A. Corma, *Chem. Sci.*, 2015, **7**, 102.
12 K. Na, C. Jo, J. Kim, K. Cho, J. Jung, Y. Seo, R. J. Messinger, B. F. Chmelka and R. Ryoo, *Science*, 2011, **333**, 328.
13 Y. Zhu, Z. Hua, X. Zhou, Y. Song, Y. Gong, J. Zhou, J. Zhao and J. Shi, *RSC Adv.*, 2013, **3**, 4193.
14 W. Ying, E. Tanja, P. Krijin and J. Zečević, *Chem. Soc. Rev.*, 2015, **44**, 7234.
15 H. Chen, J. Wydra, X. Zhang, P. Lee, Z. Wang, W. Fan and M. Tsapatsis, *J. Am. Chem. Soc.*, 2013, **133**, 12390.
16 Y. Zhang, K. Zhu, X. Duan, P. Li, X. Zhou and W. Yuan, *RSC Adv.*, 2014, **4**, 14471.
17 P. Wu, M. Yang, W. Zhang, S. Xu, P. Tian and Z. Liu, *Chem. Commun.*, 2017, **53**, 4985.
18 M. Choi, K. Na, J. Kim, Y. Sakamoto, O. Terasaki and R. Ryoo, *Nature*, 2009, **461**, 246.
19 K. Na, C. Jo, J. Kim, W. Ahn and R. Ryoo, *ACS Catal.*, 2011, **1**, 901.
20 T. Zhang, X. Chen, G. Chen, M. Chen, R. Bai, M. Jia and J. Yu, *J. Mater. Chem. A*, 2018, **6**, 9473.
21 D. Wang, L. Zhang, L. Chen, H. Wu and P. Wu, *J. Mater. Chem. A*, 2015, **3**, 3511.
22 K. A. Tarach, J. Martinez-Triguero, F. Rey and K. Góra-Marek, *J. Catal.*, 2016, **339**, 256.
23 Y. Wang, M. Lin and A. Tuel, *Microporous Mesoporous Mater.*, 2007, **102**, 80.

24 N. Wilde, M. Pelz, S. Gebhardt and R. Gläser, *Green Chem.*, 2015, **17**, 3378.
25 T. Ge, Z. Hua, J. Lv, J. Zhou, H. Guo, J. Zhou and J. Shi, *CrystEngComm*, 2017, **19**, 1370.
26 Y. Cheneviere, F. Chieux, V. Caps and A. Tuel, *J. Catal.*, 2010, **269**, 161.
27 A. Kumar, D. Srinivas, P. Pizarro, I. Moreno and S. Medina, *J. Catal.*, 2012, **293**, 126.
28 J. Li, J. Li, Z. Zhao, X. Fan, J. Liu, Y. Wei, A. Duan, Z. Xie and Q. Liu, *J. Catal.*, 2017, **352**, 361.
29 L. Wang, J. Sun, X. Meng, W. Zhang, J. Zhang, S. Pan, Z. Shen and F. Xiao, *Chem. Commun.*, 2014, **50**, 2012.
30 J. Groen, L. Peffer, J. Moulijn and J. Pérez-Ramírez, *Microporous Mesoporous Mater.*, 2004, **69**, 29.